Supplementary information

Amorphous 3D nanoflake array-assembled porous 2D cobalt-oxalate coordination polymer thin sheets with excellent pseudocapacitive performance

Lingyun Chen*[a,b], Qing Zhang[a], Hong Xu[a], Xiaohuan Hou[a], Liying Xuan[a], Yuqian Jiang[a] and Yuan Yuan[a]

[a] Department of Applied Chemistry, School of Chemistry and Chemical Engineering, Chongqing University, Chongqing 400044, China. E-mail: lychen@cqu.edu.cn

[b] State Key Laboratory of Coordination Chemistry, Nanjing University, Nanjing 210093, China

Experimental

All chemicals used in our experiments were analytical grade and were used as received without further purification.

In a typical procedure, 0.001 mol cobalt (II) nitrate hexahydrate ($Co(NO_3)_2 \cdot 6H_2O$) and 0.001 mol oxalic acid (OA) were added into 40 mL distilled water, followed by ultrasonics for 30 min. The resulting solution was transferred into a 50 mL of Teflon-lined autoclave, which was maintained at 200 °C for 24 h under electro-magnetic stirring for 500 rpm and then cooled to room temperature naturally. A pink colour product was collected by centrifuging and washed with water and absolute ethanol several times. Subsequently, these precipitates were frozen for 2 h followed by freeze-drying overnight for further characterizations. Such obtained product was designated as CQU-Co-OA-1-1.

Elemental analysis of CQU-Chen-OA-Co-1-1 ($C_2H_4O_6Co = Co(C_2O_4)(H_2O)_2$).

Calcd.: C, 13.13; H, 2.20; O, 52.46; Co, 32.21;

Found: C, 14.05; H, 2.19.

Characterization

Element analysis was carried out on Exter Analytical CE440 element analysis equipment. The crystal structure of the products were characterized by powder X-ray diffraction (XRD, Bruker D8 Advance X-ray diffract meter) using nickel-filtered Cu Kα radiation (λ = 1.5406 Å). Fourier

transform infrared (FT-IR) spectra were recorded in the range 400-4000 cm^{-1} on a Thermo Nicolet Magna IR 550II FT-IR spectrometer. The morphology and microstructures of the samples were investigated by field-emission scanning electron microscopy (SEM, HITACHI S-4800 electron microscopy) with energy-dispersive X-ray (EDX) spectra at an accelerating voltage of 20 kV. N_2 adsorption–desorption isotherms were performed on a Coulter SA-3100 analyzer apparatus with nitrogen as the analysis gas. Surface areas were calculated by the BET method and pore-size distribution was analyzed using the Barret–Joyner–Halenda (BJH) method. Thermogravimetric-differential thermal analysis (TGA-DTA) was carried out on a SHIMADZU DTG-60H simultaneous thermal analyzer.

Electrochemical measurements

All the electrochemical experiments were carried out with a CHI 660E electrochemical workstation (Chenhua Corp., Shanghai, China). A three-electrode system was employed in all the electrochemical experiments.

The working electrode was made of as-prepared CQU-Chen-OA-Co-1-1 (80 wt %), acetylene black (15 wt %) and polytetrafluoroethylene (PTFE) binder (5 wt %). After grinding, the mixed materials were pasted onto a piece of nickel foam under a pressure of 5.0 MPa and dried under vacuum at 60 °C for 12 h. Platinum wire and standard calomel electrode (SCE) were used as the counter and reference electrodes, respectively.

Electrochemical calculations

(1) Specific capacitances derived from charge–discharge tests can be calculated from the following equation:

$$C = \frac{I \times \Delta t}{m \times \Delta V} \qquad ①$$

where C ($F\ g^{-1}$) is the specific capacitance of the electrode based on the mass of active materials, I (A) is the current during discharge process, Δt (s) is the discharge time, ΔV (V) is the potential window (here ΔV = 0.5 V), m (g) is the mass of active materials.

(2) Energy density and power density derived from charge–discharge tests can be calculated from the following equations:

$$E = \frac{1}{2} C V^2 \qquad ②$$

$$P = \frac{E}{t} \qquad ③$$

where E (Wh kg^{-1}) is the average energy density; C (F g^{-1}) is the specific capacitance; V (V) is the potential window (here ΔV = 1.5 V); P (W kg^{-1}) is the average power density and t (s) is the discharge time.

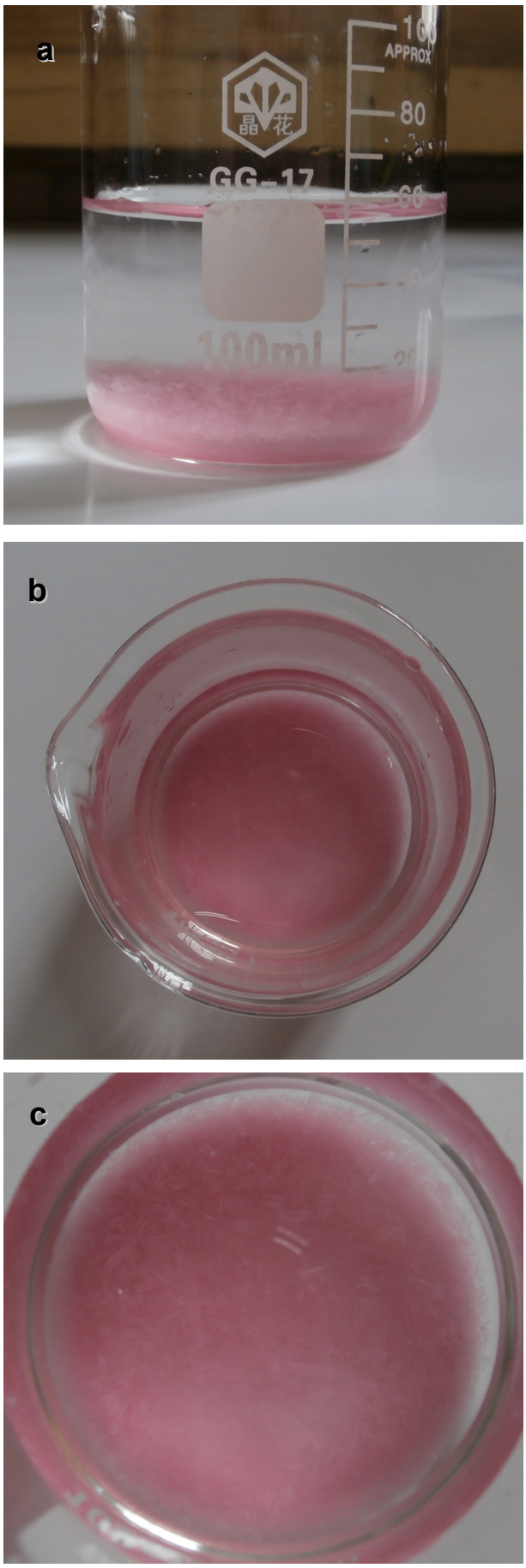

Fig. S1 (a)-(c) Digital photography of the CQU-Chen-Co-OA-1-1 (a) and (b) in 100 ml beaker after hydrothermal reaction at 200°C for 24 h.

Fig. S2 Digital photography of the CQU-Chen-Co-OA-1-1 after freeze-drying.

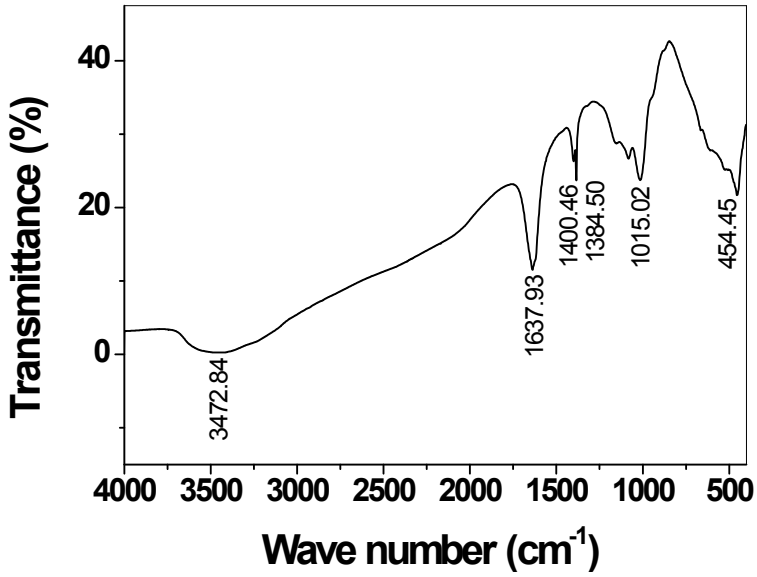

Fig. S3 Fourier transforms infrared spectra (FT-IR) of the CQU-Chen-Co-OA-1-1.

FT-IR analysis: The FT-IR spectrum of CQU-Chen-OA-Co-1-1 in Fig. S3) shows the broad band above 3400 (between 3100 and 3600) cm^{-1} which is attributed to asymmetric and symmetric stretching of OH^- and the absorbed H_2O molecule. This band is related to moisture in the sample. And the absorbed H_2O bending vibration also appears at 1400 cm^{-1}. The stretching band of carbonyl group ν(C=O) at 1638 cm^{-1}, the stretching band of C–O bond ν(C–O) at 1385 cm^{-1}, the O–C=O out of plane bending mode δ(O–C=O) of oxalate at 776 cm^{-1} and

the O–C=O in-plane bending mode δ(O–C=O) at 510 cm^{-1}. And the frequencies of Co–O bonds ν(Co–O) can be seen at 454 cm^{-1}.

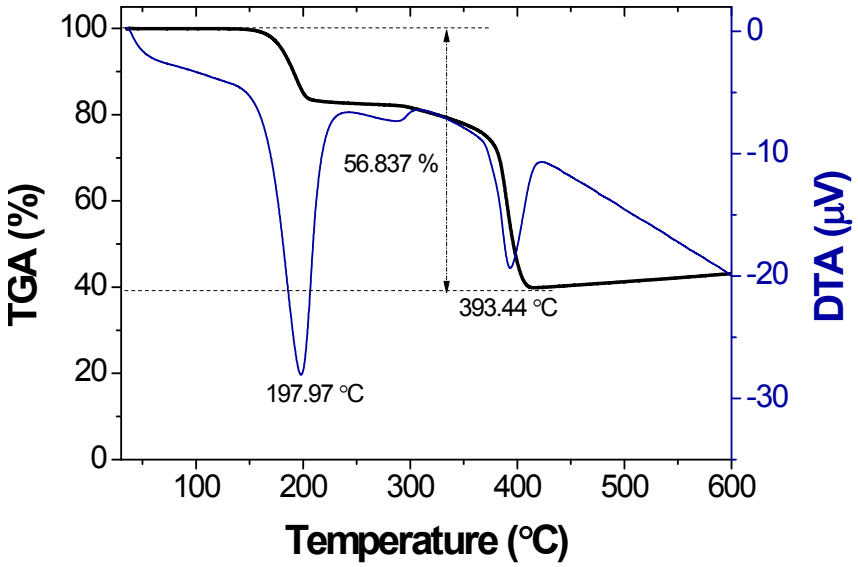

Fig. S4 Thermogravimetric-differential thermal analysis (TGA-DTA) curves of the CQU-Chen-Co-OA-1-1 in the range between room temperature (25 °C) and 600 °C with Air flow rate of 100 mL/min at a heating rate of 10°C/min in air atmosphere.

TGA-DTA analysis: The thermal behaviour of the CQU-Chen-OA-Co-1-1 has been examined using thermogravimetric-differential thermal analysis (TGA-DTA) in Fig. S4. It seems that the decomposition proceeds in two stages. The first 20.76 % weigh loss exhibited a weight change below 200 °C associated with the dehydration of crystal water, and the second 36.08 % weigh loss seems to be related to the greater decomposition step above 400 °C corresponds to the decomposition of $C_2O_4^{2-}$ anion degradation with CO and CO_2 evolution due to the chemical reaction between [$Co(C_2O_4)$] and O_2. The relatively high thermal decomposition temperature shows that CQU-Chen-OA-Co-1-1 has good thermal stability properties.

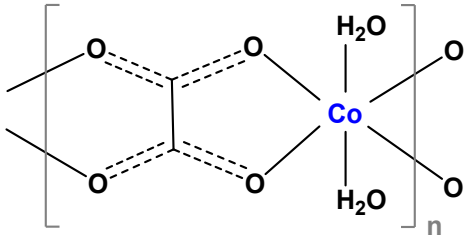

Fig. S5 The structure of the $[Co(\mu\text{-}ox)(H_2O)_2]_n$ CPs.

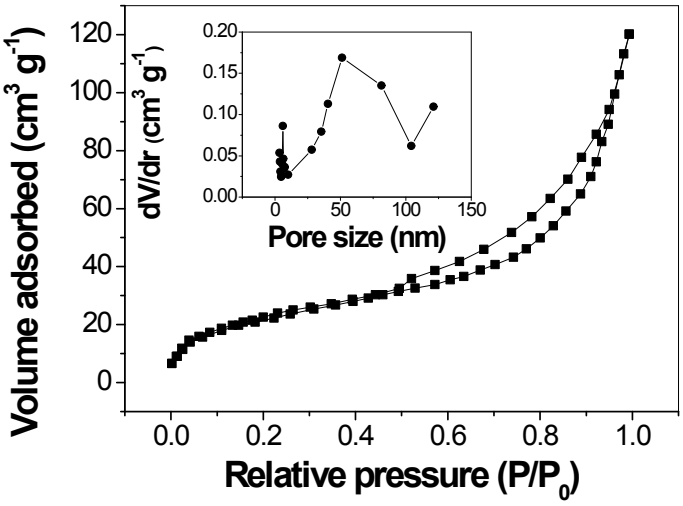

Fig. S6 N_2 adsorption/desorption isotherms and the pore-size distribution plot of the CQU-Chen-OA-Co-1-1.